A study of the valence shell electronic states of s-triazine by photoabsorption spectroscopy and ab initio calculations

D.M.P. Holland [a,⇑], D.A. Shaw [a], M. Stener [b,c,d], P. Decleva [b,c,d], S. Coriani [b,c,e]

[a] Daresbury Laboratory, Daresbury, Warrington, Cheshire WA4 4AD, UK
[b] Dipartimento di Scienze Chimiche e Farmaceutiche, Università degli Studi di Trieste, Via L. Giorgieri, I-34127 Trieste, Italy
[c] Consorzio Interuniversitario Nazionale per la Scienze e Tecnologia dei Materiali, INSTM, Unità di Trieste, Italy
[d] CNR-IOM, Trieste, Italy
[e] Aarhus Institute of Advanced Studies, Aarhus University, 8000 Aarhus C, Denmark

a b s t r a c t

The absolute photoabsorption cross section of s-triazine has been measured between 4 and 40 eV, and is dominated by bands associated with valence states. Structure due to Rydberg excitations is both weak and irregular. Jahn-Teller interactions affect the vibronic structure observed in the Rydberg absorption bands due to excitation from the $1e^{00}$ or $6e^{0}$ orbitals. The interpretation of the experimental spectrum has been guided by transition energies and oscillator strengths, for Rydberg and valence states, calculated with the time-dependent version of density functional theory and with the coupled cluster linear response approach. The theoretical studies indicate that Rydberg/Rydberg and Rydberg/valence mixing is important.

1. Introduction

The valence shell photoabsorption spectrum of 1,3,5 (sym) – tri-azine ($C_3N_3H_3$), henceforth abbreviated to s-triazine, is dominated by broad bands due to transitions into excited valence states. In contrast, structure due to Rydberg states, which is already weak in the diazines ($C_4N_2H_4$) [1,2], is reduced further in intensity through the introduction of an additional nitrogen atom. This evi-dent simplicity in the valence electronic structure has resulted in s-triazine being included in the group of molecules whose low-lying excited states are being used to evaluate the suitability of various theoretical approaches to the calculation of vertical transition energies [3–5]. In comparison with the diazines, where the excited electronic states (valence and Rydberg) are reasonably understood, much less is known about the corresponding states in s-triazine, and experimental measurements of the photoabsorption spectrum are limited to energies below 11.5 eV [6]. The aim of the present study is to improve our knowledge of the valence shell electronic states by extending the absorption measurements to encompass the entire valence shell (up to 40 eV) and by calculating vertical transition energies and oscillator strengths.

According to our recent work on the photoelectron spectrum of s-triazine [7], the ground state outer valence electronic configura-tion (D_{3h} symmetry) may be written as:

ð4a1⁰ðrÞ² ð1a2⁰ðrÞ² ð1a2⁰⁰ð1pÞ² ð5e⁰ðrÞ⁴ ð5a1⁰ðnNÞ² ð1e⁰⁰ð2pÞ⁴
ð6e ðnNÞ X A1

where n_N denotes a non-bonding orbital associated with a nitrogen atom.

The virtual valence p′ orbitals are $2e^{00}(1p')$ and $2a^{00}{}_2(2p')$, so the lowest valence transitions are expected to be $6e^{0}$? $2e^{00}(n_N$? $1p', 1A^{00}{}_2)$, $1e^{00}$? $2e^{00}(2p$? $1p', 1E^{0})$ and $1e^{00}$? $2a^{00}{}_2(2p$? $2p', E^{0})$, while the other valence transitions from the inner (p or r) orbitals, $1a^{00}{}_2$? $2e^{00}(1p$? $1p', E^{0})$ and $5e^{0}$? $2e^{00}(r$? $1p', A^{00}{}_2)$, are expected at higher energies.

Early experimental photoabsorption studies, reviewed compre-hensively by Innes et al. [8], concentrated on the singlet excited states of $A^{00}{}_1$, $A^{00}{}_2$ or E^{00} symmetry arising from the $6e^{0}(n_N)$? $2e^{00}$ (p′) transition [9–14]. The adiabatic transition into the one-photon forbidden $^1E^{00}$ electronic state lies at 3.8 eV [11], and that into the allowed $^1A^{00}{}_2$ state at slightly higher energy [11,14]. Subsequent measurements encompassed the intense absorption band, due principally to transitions into valence states, at 7.8 eV [6]. How-ever, little is known about the higher-lying valence states even though, as will be shown in the present work, such states consti-tute the largest contribution to the valence shell photoabsorption spectrum.

Only fragmentary information is currently available on the absorption bands associated with Rydberg excitations. This is due, at least in part, to the inadequate resolution employed in pre-vious single-photon absorption studies. Another factor hampering

⇑ Corresponding author.
E-mail address: david.holland@stfc.ac.uk (D.M.P. Holland).

the identification of the Rydberg absorption bands is configuration interaction. Our theoretical studies indicate that many of the Ryd-berg states mix strongly with valence or other neighbouring Ryd-berg states. Such perturbations often lead to shifts in transition energies and to irregular intensity distributions, and, consequently, to the apparent loss of features expected simply on the basis of the Rydberg formula.

The exception to this general lack of information concerning Rydberg states is that due to the $6e^0$? $3sa^0{}_1\ {}^1E^0$ excitation. The vibronic structure associated with this state, which is affected by Jahn-Teller interactions [15,16], has been studied in detail using two-photon absorption spectroscopy [17,18].

2. Experimental apparatus and procedure

The absolute photoabsorption cross section of s-triazine was measured using two experimental chambers – a cell incorporating LiF windows [19], and a double ion chamber [20] – and syn-chrotron radiation emitted from the Daresbury Laboratory storage ring [21]. In both cases the experimental chamber was attached to a 5 m normal incidence monochromator which delivers radiation in the energy range of 5–45 eV [22]. In the present experiment a photon resolution of 0.1 nm FWHM (5 meV at hm = 8 eV) was employed.

The windowed cell allowed the photoabsorption cross section to be obtained through application of the Beer-Lambert law, $I_t = I_0\exp(-nrl)$, where I_t is the intensity of the transmitted radia-tion after passing through the gas column, I_0 is the corresponding incident intensity, n is the gas number density, r is the photoab-sorption cross section and l is the length of the gas column. Spectra were recorded using gas pressures in the 5–30 lbar range. The experimental uncertainty associated with the determination of absolute photoabsorption cross sections using this cell is estimated as 5% [19]. The photon energy scale was calibrated by recording high resolution absorption spectra of a gas mixture comprising s-triazine, nitrous oxide and nitric oxide [1,2,23].

At photon energies above 11.8 eV (the LiF cutoff), the absolute photoabsorption cross section was measured with the double ion chamber [20]. The possible influence of scattered light or second order radiation on the photoabsorption spectrum using this arrangement has been discussed in detail previously [2,20,24]. Such contributions are expected to have negligible effects. The photon energy scale was calibrated by recording high resolution spectra of a gas mixture comprising s-triazine, argon and xenon [2].

3. Theoretical approach

3.1. Density functional theory

The time-dependent version of density functional theory (TDDFT) was employed to calculate the total valence shell pho-toabsorption cross section of s-triazine [25]. Below the ionisation threshold, the spectrum was calculated using the ADF code [26] with a (9s, 7p, 5d, 4f) even-tempered basis set consisting of Slater-type orbitals (indicated as ET-QZ3P-3DIFFUSE in the ADF data-base). Preliminary test calculations with larger basis sets did not show appreciable changes in the results below the ionisation threshold, thereby indicating that the basis set had been chosen properly. In the calculations, we have considered not only the opti-cally allowed singlet-singlet transitions but also the lowest elec-tric-dipole-forbidden transitions. The computed excitation energies correspond to vertical transitions.

Above the ionisation limit, the proper boundary conditions of the continuum spectrum have to be taken into account. Therefore, in this energy region, we have employed the TDDFT approach implemented with multicentre B-spline basis functions [27]. The other computational details are similar to those given previously [28]. It should be noted that the LB94 [29] exchange-correlation potential has been used since it supports the correct asymptotic behaviour. This has been shown to be important in generating accurate TDDFT spectra [30], as well as continuum cross section profiles [31].

Table 1 reports the LB94 binding energies of the occupied and the virtual orbitals, in addition to giving a short description of the orbital nature. These binding energies represent the starting point in the description of the electronic structure, and have been used to calculate the valence photoabsorption.

To simplify the comparison between experiment and theory, the discrete excitations below the ionisation threshold (Table 2) have been convoluted with Gaussian functions of 0.5 eV (FWHM), while the continuum cross section profile has been convoluted with Gaussian functions of 2.0 eV (FWHM) to smooth the very nar-row peaks associated with the many autoionising Feshbach reso-nances. The width (0.5 eV) of the Gaussian broadening used to convolute the discrete excitations was chosen in order to repro-duce the observed widths (due essentially to vibrational envelopes).

3.2. Coupled cluster approach

Coupled cluster linear response theory [33] was used to com-pute the excitation energies and oscillator strengths of the dipole allowed transitions up to around 11 eV. The calculations employed a Coupled Cluster Singles and Doubles (CCSD) wavefunction [34], together with a modified version of Dunning's correlation

Table 1
Binding energies of occupied and virtual valence orbitals of s-triazine calculated with the DFT approach.

Orbital[a]	Binding energy (eV)	
	Theory[b]	Experiment
Occupied		
$3a_1{}^0$(r)	30.71	30.7 [7]
$3e^0$ (r)	27.49	27.5 [7]
$4e^0$ (r)	22.09	22.2 [7]
$1a_2{}^0$(r)	18.90	17.6 [32]
$4a_1{}^0$(r)	18.81	18.31 [32]
$1a_2{}^{00}$(p)	17.12	14.99 [32]
$5e^0$ (r)	15.79	14.64 [32]
$5a_1{}^0$(nN)	14.26	13.37 [32]
$1e^{00}$(p)	14.17	11.79 [32]
$6e^0$ (nN)	11.83	10.40 [32]
Virtual		
$2e^{00}$(p′)	8.38	
$2a_2{}^{00}$(p′) r	4.55	
$6a^{\upsilon}$ (Ryd 3s, ′)	4.45	
$7e^0$ (Ryd 3px, 3py, r′)	3.73	
$7a^0$ (Ryd 3d $_{z^2}$)	3.59	
$3a^{\upsilon\upsilon}_{2}$ (Ryd 3p)$_z$	2.93	
$8e^0$ (Ryd 3px, 3py)	2.64	
$3e^{00}$(Ryd 3dxz)	1.99	
$2a^{\upsilon}$	1.33	
$8a^{\upsilon}$	1.20	
$9e^{\upsilon}$	0.95	
$4a^{00}$	0.82	
$9a^{\upsilon}$	0.81	
$10e^{\upsilon}$	0.63	
$4e^{00}$	0.57	
$11e^0$	0.51	

[a] r, p or nN is used to label the orbital bonding character, where nN denotes a non-bonding orbital on the nitrogen atom.

[b] LB94 eigenvalues obtained with the ET-QZ3P-3DIFFUSE basis set. Absolute values are reported for the occupied orbitals.

Table 2
Valence electron electric-dipole allowed singlet-singlet excitations in s-triazine calculated with the TDDFT approach.

Transition[a]	Excitation energy (eV)[b]	Oscillator strength (f 10^2)	Assignment[c]
1 $^1A_2^{00}$	3.70	0.85	100% $6e^0$? $2e^{00}$
1 $^1E^0$	7.38	1.31	93% $6e^0$? $6a_1^0$(3s, r)
2 $^1A_2^{00}$	7.58	0.27	100% $5e^0$? $2e^{00}$
2 $^1E^0$	7.65	67.99	85% $1e^{00}$? $2e^{00}$
3 $^1E^0$	8.12	14.04	100% $6e^0$? $7e^0$(3px, 3py, r)
4 $^1E^0$	8.30	4.18	99% $6e^0$? $7a_1^0$($3dz^2$)
5 $^1E^0$	9.15	0.62	62% $1a_2^{00}$? $2e^{00}$
			19% $1e^{00}$? $2a_2^{00}$
			17% $6e^0$? $8e^0$(3px, 3py)
6 $^1E^0$	9.24	7.10	82% $6e^0$? $8e^0$(3px, 3py)
3 $^1A_2^{00}$	9.80	0.61	99% $6e^0$? $3e^{00}$(3dxz)
4 $^1A_2^{00}$	10.11	2.30	96% $5a^{00}$? $2a^{00}$
5 $^1A_2^{00}$	10.47	2.96	100% $1e^{00}$? $7e^0$(3px, 3py, r)
7 $^1E^0$	10.49	7.47	99% $6e^0$? $2a_2^0$
8 $^1E^0$	10.54	0.09	64% $5a_1^0$? $7e^0$(3px, 3py, r)
			24% $6e^0$? $8a_1^0$
9 $^1E^0$	10.61	3.43	58% $6e^0$? $8a_1^0$
			33% $5a_1^0$? $7e^0$(3px, 3py, r)
10 $^1E^0$	10.78	3.03	32% $1e^{00}$? $2a_2^{00}$
			20% $6e^0$? $9e^0$
			15% $6e^0$? $8a_1^0$
			15% $1e^{00}$? $3a_2^{00}$(3pz)
			10% $1a_2^{00}$? $2e^{00}$
11 $^1E^0$	10.92	4.13	78% $6e^0$? $9e^0$
12 $^1E^{00}$	11.03	5.72	98% $6e^{00}$? $9a^{00}$
13 $^1E^0$	11.21	2.16	97% $6e^{00}$? $10e^{00}$
6 $^1A_2^{00}$	11.22	3.32	99% $6e^0$? $4e^{00}$
14 $^1E^0$	11.34	0.18	66% $6e^0$? $11e^0$
			19% $5e^0$? $6a_1^0$(3s, r)
			10% $1e^{00}$? $3a_2^{00}$(3pz)
7 $^1A_2^{00}$	11.36	0.30	98% $5a_1^0$? $3a_2^{00}$(3pz)
15 $^1E^0$	11.38	9.32	34% $5e^0$? $6a_1^0$(3s, r)
			23% $1e^{00}$? $3a_2^{00}$(3pz)
			31% $6e^0$? $11e^0$
16 $^1E^{00}$	11.43	0.49	87% $6e^{00}$? $10a^{00}$
17 $^1E^0$	11.47	13.84	40% $5e^0$? $6a_1^0$(3s, r)
			33% $1e^{00}$? $3a_2^{00}$(3pz)
8 $^1A_2^{00}$	11.61	3.17	99% $1e^{00}$? $8e^{00}$(3px, 3py)
18 $^1E^0$	11.66	0.03	98% $6e^0$? $11a_1^0$
19 $^1E^0$	11.74	0.67	78% $6e^0$? $12e^0$
			18% $5a_1^0$? $8e^0$(3px, 3py)
20 $^1E^0$	11.77	0.09	64% $5a_1^0$? $8e^0$(3px, 3py)
			21% $6e^0$? $12e^0$
9 $^1A_2^{00}$	11.77	0.06	100% $6e^{00}$? $5e^{00}$
21 $^1E^0$	11.83	0.00	94% $6e^0$? $13e^0$
22 $^1E^0$	11.90	0.04	99% $6e^0$? $12a_1^0$

[a] Calculations performed at the TDDFT level using the ADF programme with the ET-QZ3P-3DIFFUSE basis set. All transitions are reported for excitation energies up to 12 eV.

[b] Calculated energies correspond to vertical transitions.

[c] Assignments are given in terms of the leading one-electron excited configurations.

consistent aug-cc-pVTZ basis set [35], where the f functions on the second row atoms were removed. We label this basis set as aug-cc-pVTZ-f. In order to improve on the basis set convergence and on the description of the Rydberg states, the basis set was supple-mented with a set of (3s3p3d) molecule-centred primitive basis functions constructed according to Kaufmann et al. [36], with quantum number n = 3, 3.5, 4. Ionisation energies were computed using the aug-cc-pVTZ-f basis set at both the CCSD level and using the non-iterative method known as CCSDR(3) [37]. In the latter method, the single replacement dominated excitations are correct through third order in the fluctuation potential, and the double replacement dominated excitations are correct through second order. All the coupled cluster calculations were performed using a local version of the Dalton program [38], and the results are col-lected in Tables 3 and 4, for the ionisation and absorption data, respectively.

4. Results and discussion

4.1. Overview of the total photoabsorption spectrum

The experimental valence shell absolute photoabsorption cross section of s-triazine is plotted in Fig. 1, together with the convo-luted TDDFT results. The calculated partial final continuum contri-butions are also shown and, throughout the energy range covered in the present experiment, the largest contribution corresponds to that having e^0 symmetry. Our experimental spectrum represents the first measurement of the absolute photoabsorption cross sec-tion of s-triazine above an energy of 11.5 eV. The general shape of our spectrum is similar to that reported by Walker et al. [6], but the absolute values are lower. This difference is particularly noticeable in the intense band at 7.8 eV, where our peak maxi-mum of 120 Mb is considerably lower than that (165 Mb) of Walker et al. However, our values are consistent with those of the corresponding peaks in the diazines [1,2], and indeed consis-tent with expectations based on oscillator strength sum rules.

In the high energy range of the spectrum reported in Fig. 1, the TDDFT profile appears shifted by about 2 eV to lower energy, and to have a slightly underestimated intensity, with respect to the experimental result. This discrepancy is a characteristic of the TDDFT method since a similar behaviour has been observed in other molecules (in particular, benzene and the diazines) see, for example, Fig. 8 in Ref [2]. We attribute this effect to a deficiency of the LB94 exchange-correlation potential, which is too attractive and therefore tends to shift the profiles to lower energy [31].

4.2. Valence states

Fig. 2(a) and (b) shows the experimental photoabsorption cross section between 3.6 and 12.1 eV, together with the theoretically predicted intravalence and Rydberg transitions obtained with the CCSD (Table 4) and TDDFT (Table 2) methods. Tables 2 and 4 list the excited state vertical ionisation energies, oscillator strengths and assignments in terms of the leading one-electron excited con-figurations. In general, the present vertical ionisation energies for the low-lying valence states agree to within a few tenths of an eV with the values obtained in the benchmark [3–5] and other

Table 3
Valence ionisation energies of s-triazine, as computed at the CCSD and CCSDR(3) levels of theory, using basis sets aug-cc-pVTZ on H, and aug-cc-pVTZ minus f functions on C and N.

Symmetry		Ionisation energy (eV)		
D_{3h}	C_{2v}	CCSD (%T_1)[a]	CCSDR(3)	Experiment
$6e^0$(nN)	$A_1 + B_1$	10.38 (94.5)	10.34	10.40 [32]
$1e^{00}$(p)	$B_2 + A_2$	11.94 (94.9)	11.94	11.79 [32]
$5a_1^0$ (nN)	A_1	13.43 (92.3)	13.28	13.37 [32]
$5e^0$(r)	$A_1 + B_1$	15.29 (94.9)	15.13	14.64 [32]
$1a_2^{00}$ (p)	B_2	15.63 (91.5)	15.35	14.99 [32]
$1a_2^0$ (r)	B_1	18.40 (93.7)	18.50	17.6 [32]
$4a_1^0$ (r)	A_1	18.80 (92.4)		18.31 [32]
$4e^0$(r)	$A_1 + B_1$	22.37 (64.1)		22.2 [7]
	$A_1 + B_1$	22.67 (26.6)		

[a] The symbol %T_1 in parenthesis indicates the percentage of ‘single excitation’ character of the given ionisation.

Table 4
Dipole-allowed valence electron excitations in s-triazine as computed at the CCSD level of theory.

Transition[a]	Excitation energy (eV)[b]	Oscillator strength (f 10^2)	Assignment[c]
1 $^1A_2^{00}$	5.00	1.66	$6e^0$? $2e^{00}$
1 $^1E^0$	7.33	4.63	$6e^{U}$? $3s(a^{U}_1)$
2 $^1E^0$	8.12	43.9	$6e^{U}$? $3p_{x,y}(e^{U})$ + $1e^{UU}$? $2e^{UU}$
3 $^1E^0$	8.31	58.2	$1e^{00}$? $2e^{00}$
4 $^1E^0$	8.53	1.05	$6e^0$? $3d_{z^2}$ ($a1^0$)
5 $^1E^0$	8.80	1.08	$6e^0$? $3d_{xy;x^2-y^2}$ (e^0)
2 $^1A_2^{00}$	8.86	1.16	$6e^0$? $3d_{xz,yz}(e^{00})$ + $6e^0$? $2e^{00}$
6 $^1E^0$	9.04	1.13	$6e^{U}$? $4s(a^{U}_1)$
7 $^1E^0$	9.31	0.46	$6e^{U}$? $4p_{x,y}(e^{U})$
8 $^1E^0$	9.40	0.52	$6e^0$? $4d_{z^2}$ ($a1^0$)
3 $^1A^{00}_2$	9.50	0.98	$5e^{U}$? $2e^{UU}$
9 $^1E^0$	9.53	1.02	$6e^0$? $4d_{xy;x^2-y^2}$ (e^0)
4 $^1A_2^{00}$	9.56	0.79	$6e^0$? $4d_{xz,yz}(e^{00})$ + $6e^0$? $2e^{00}$
10 $^1E^U$	9.61	0.26	$6e^{U}$? $5s(a^{U}_1)$
11 $^1E^0$	9.62	0.08	$1e^{00}$? $3p_z(a_2^{00})$ + $1e^{00}$? $2e^{00}$
5 $^1A_2^{00}$	9.67	4.09	$1e^{00}$? $3p_{x,y}(e^0)$ + $3d_{xy;x^2-y^2}$ (e^0)
12 $^1E^0$	9.80	0.73	$6e^0$? $5p_{x,y}(e^0)$ + $5d_{xy;x^2-y^2}$ (e^0)
13 $^1E^0$	9.88	0.56	$6e^0$? $5d_{z^2}$ ($a1^0$)
14 $^1E^0$	10.01	0.001	$6e^0$? $5s(a1^0)$ + $5d_{z^2}$ ($a1^0$) + 4f
15 $^1E^0$	10.06	7.05	$6e^0$? $5d_{xy;x^2-y^2}$ (e^0) + $6e^0$? a_2^0 (valence)
16 $^1E^0$	10.17	0.69	$6e^0$? $5d_{xy;x^2-y^2}$ (e^0) + $6e^0$? a_2^0 (valence)
6 $^1A_2^{00}$	10.17	0.86	$6e^0$? $5d_{xz,yz}(e^{00})$ + $6e^0$? $2e^{00}$
7 $^1A_2^{00}$	10.41	0.29	$1e^{00}$? $3d_{xy;x^2-y^2}$ (e^0)
17 $^1E^0$	10.51	5.10	$1a_2^{00}$, $1e^{00}$? $2e^{00}$
18 $^1E^0$	10.81	0.61	$1e^{00}$? $4p_z(a_2^{00})$
8 $^1A_2^{00}$	10.85	1.62	$1e^{00}$? $4p_{x,y}(e^0)$ + $4d_{xy;x^2-y^2}$ (e^0)
19 $^1E^0$	11.14	0.06	$1e^{00}$? $4d_{xz,yz}(e^{00})$

[a] Calculations performed using the aug-cc-pVTZ basis set on H, the aug-cc-pVTZ minus f functions basis set on C and N, plus a set (3s3p3d) of Rydberg-type func-tions in the centre of mass.
[b] Calculated energies correspond to vertical transitions.
[c] Assignments are given in terms of the leading one-electron excited configurations.

theoretical [6,39–41] studies. Although both theoretical approaches employed in our work provide a broadly satisfactory description of the valence shell photoabsorption spectrum of s-tri-azine, we discuss the transitions into the low-lying valence and Rydberg states in relation to the CCSD predictions, and use the TDDFT results to interpret the entire spectrum over an extended energy range. Despite the slightly more pronounced shift in the calculated transition energies, compared to the experimental val-ues, we consider the CCSD results more dependable than the TDDFT predictions, due to the inclusion of a description of double excitations within the CCSD approach.

According to our CCSD calculations (Table 4), the lowest-lying, electric-dipole-allowed transition, $6e^0(n_N)$? $2e^{00}(\pi^*)$ $^1A^{00}_2$, occurs at 5.00 eV. The corresponding absorption band, whose maximum lies at 4.6 eV, has been studied extensively [8,10,13,14]. This valence state, 1 $^1A^{00}_2$, gives rise to a weak band in the present spec-trum, in accord with previous investigations.

The next optically allowed transition into a state containing sig-nificant valence character, 2 $^1E^0$, is separated from that associated with the 1 $^1A^{00}_2$ state by 3 eV. Our spectrum exhibits a weak absorption band around 5.6 eV and a gradual increase in intensity at about 6.5 eV. It is conceivable that the forbidden $1e^{00}(\pi)$? $2e^{00}$ (π^*) 1 ^1A $^0_2$ and $1e^{00}(\pi)$? $2e^{00}(\pi^*)$ 2 $^1A^0_1$ transitions, predicted at 5.92 and 6.90 eV by our TDDFT calculations (not reported), may account for these features.

Two intense transitions, both of E^0 symmetry, are predicted around 8 eV (Table 4). The first, at 8.12 eV, has a mixed

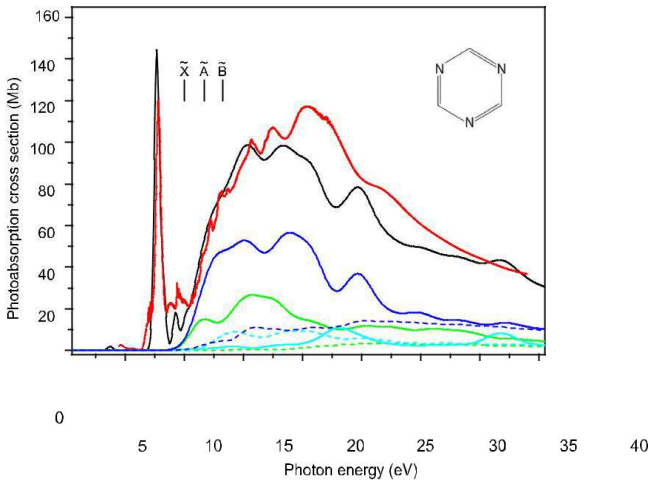

Fig. 1. The experimental (red) and convoluted TDDFT (black) photoabsorption cross section of s-triazine. The calculated partial final continuum contributions (—a^0_1 (green), —a^0_2 (cyan), —e^0(blue), - - -a^{00}_1 (green), - - -a^{00}_2 (cyan), - - -e^{00}(blue)) are shown.

The X E , A E and B A_1 state ionisation limits at 10.01, 11.69 and 13.26 eV [45], respectively, are marked. (For interpretation of the references to colour in this figure legend, the reader is referred to the web version of this article.)

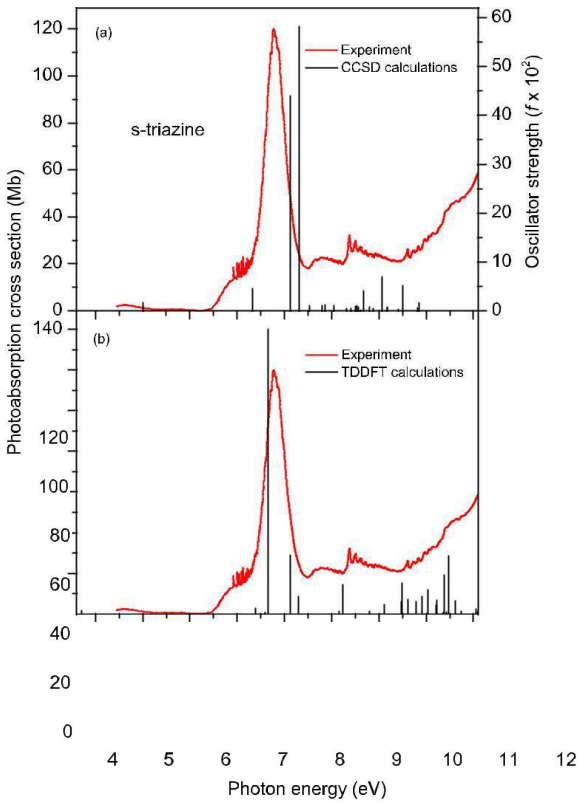

Fig. 2. (a) The experimental photoabsorption cross section of s-triazine (red) and the CCSD predicted oscillator strengths (black), plotted as vertical bars, using the results given in Table 4. (b) The experimental photoabsorption cross section of s-triazine (red) and the TDDFT predictions (black), plotted as vertical bars, using the results given in Table 2. (For interpretation of the references to colour in this figure legend, the reader is referred to the web version of this article.)

Rydberg/valence character and arises from the $6e^0(n_N)$? $3p_{x,y}(e^0)$ and $1e^{00}(\pi)$? $2e^{00}(\pi^*)$ transitions. The second, at 8.31 eV, is due to the $1e^{00}(\pi)$? $2e^{00}(\pi^*)$ valence transition. A third, and least intense, transition ($6e^0(n_N)$? $3d_{z^2}$ (a^0_1)), of purely Rydberg character, is pre-dicted at slightly higher energy. The individual contributions from

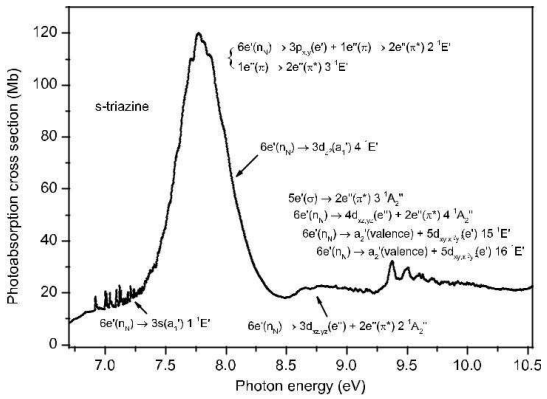

Fig. 3. Photoabsorption cross section of s-triazine, encompassing the excitation range 6.7–10.5 eV, showing the broad, intense bands due to transitions into valence states. Calculated transition energies are given in Table 4.

these three close-lying transitions cannot be distinguished but col-lectively form the peak observed at 7.8 eV (Fig. 3). This absorption band, which dominates the valence shell absorption spectrum of s-triazine, is of a similar nature to those observed in the diazines [2] and benzene [2].

The 2 $^1A''_2$ state, of mixed Rydberg/valence character, may be responsible for the broad absorption band appearing between 8.5 and 9.2 eV (Fig. 3). Another broad band, observed between 9.2 and 10.3 eV, probably correlates with the 3 $^1A''_2$, 4 $^1A''_2$, 15 $^1E^0$ and 16 $^1E^0$ states, all of which contain significant valence contributions. Interestingly, the 3 $^1A''_2$ state, with a calculated excitation energy of 9.50 eV, is predicted to arise from the $5e^0$(HOMO-3) ? $2e''(\pi')$ transition. Another state of pure valence character, and one which has a substantial oscillator strength, is that at 10.51 eV, arising from the $1a''_2,1e''$? $2e''(\pi ? \pi')$ transitions.

At higher excitation energies the density of predicted valence states increases and it becomes progressively difficult to match a specific calculated transition to an observed peak. Although a detailed interpretation of the theoretical results at these high ener-gies is unwarranted, Fig. 1 shows that the TDDFT calculations, which have been performed over an extended energy range, pro-vide a satisfactory account of the overall shape of the experimental spectrum.

4.3. Rydberg states

The normal procedure for identifying absorption bands associ-ated with transitions into Rydberg states is through use of the for-mula $E_n = E_I - 13.606/(n - \delta_l)^2$, where E_n is the transition energy for the promotion of an electron from a particular orbital into a Rydberg orbital of principal number n and E_I is the relevant ioni-sation energy. δ_l is the quantum defect of the lth series. Previous studies have established that, for a given value of l (the orbital angular momentum) δ_l generally lies within a small range and is almost independent of n for an unperturbed series. The quantum defect characterises the short-range non-Coulombic interactions between the electron and the ion core, due to the penetration of the Rydberg electron into the molecular framework. Its value has been discussed extensively [42,43], particularly in regard to small, or linear, molecules consisting of light atoms. For such molecules, δ_l is expected to have values which lie in the ranges (0.8 to 1.0), (0.4 to 0.7), (0.2 to 0.2) and (0.2 to 0.2) for ns, np, nd and nf ser-ies respectively. Quantum defects have been calculated for a range of positive atomic ions by Theodosiou et al. [44]. Assignments based upon the use of the Rydberg formula work well for unper-turbed states. However, if a Rydberg state is perturbed through interaction with an adjacent Rydberg or valence state (Rydberg/ Rydberg or Rydberg/valence mixing, respectively), then the transi-tion energy may be shifted and regular Rydberg series are no longer observed. Both our experimental spectrum and our theoret-ical results suggest that many of the Rydberg states in s-triazine are perturbed and that the excited state cannot be described ade-quately in terms of a predominantly one-electron excited configu-ration. Rather, these nominally Rydberg orbitals have a mixed Rydberg/valence or Rydberg/Rydberg character.

Many of the Rydberg states observed in the photoabsorption spectrum exhibit accompanying vibrational structure. Since the molecular geometry of a Rydberg state is generally similar to that of the ionic state onto which the series converges, the Franck-Con-don factor connecting the ground and Rydberg state is expected to be similar to that connecting the ground and corresponding ionic state. Thus, the assignments for the vibrational structure appearing in the photoabsorption spectrum may be guided through compar-ison with those for the associated photoelectron band.

The lowest-lying Rydberg state arises from the $6e^0(n_N)$? $3sa''_1$ $^1E^0$ transition (Table 4) and complex structure due to this state has been observed in previous one-photon absorption experiments [6,8,9,13]. A proper interpretation of this structure, which was not obtained in the one-photon absorption studies, was achieved through the two-photon absorption investigation on jet-cooled s-triazine performed by Whetten et al. [17,18]. Electric dipole selec-tion rules show that for transitions originating from a totally sym-metric ground state, only states of E^0 symmetry are accessible in both one- and two-photon absorption processes. Whetten et al. assigned the vibronic structure observed in the two-photon absorption spectrum using transition energies and intensities obtained from a model calculation which showed that the struc-ture resulted from the dynamical Jahn-Teller effect where only one vibrational mode, the ν_{12} ring distortion, was significantly active. Interestingly, the calculations also showed that when the ionic state onto which a Rydberg series converges is degenerate,

$\tilde{X}\,^2E^0$ $\tilde{A}\,^2E''$

as is the case for the X E and A E states of s-triazine, a nondegen-erate Rydberg state displays vibronic structure which resembles that derived from an electronic degeneracy. Thus, the observed structure is related to the Franck-Condon factor connecting the ini-tial state and the final Jahn-Teller influenced ion core, irrespective of the symmetry of the Rydberg state.

In the HeI excited photoelectron spectrum of the $\tilde{X}\,^2E^0$ state [45], the vibrational structure was assigned to excitations involv-ing the $\nu^+_{11}(e^0)$, $\nu^+_{12}(e^0)$ and $\nu^+_{14}(e'')$ modes, in addition to the totally symmetric $\nu^+_2(a''_1)$ and $\nu^+_3(a''_1)$ modes (where the Herzberg nomen-clature has been adopted for the numbering of the vibrational modes [46,47]). However, these assignments were not discussed in relation to possible Jahn-Teller effects. According to Whetten et al. [17,18], the structure in the 3s Rydberg state should be ascribed to the vibronically active ν_{12} mode, in addition to excita-tions involving the totally symmetric ν_2 and ν_3 modes. In the neu-tral ground state the ν_2, ν_3 and ν_{12} modes have calculated energies of 140.0, 121.3 and 83.7 meV, respectively [48]. Fridh et al. [45] have measured the $\tilde{X}\,^2E^0$ state adiabatic ionisation threshold as 10.01 eV.

Fig. 4 shows the photoabsorption spectrum in the energy range between 6.80 and 7.45 eV, which encompasses structure due to the $6e^0$? $3sa''_1$ $^1E^0$ Rydberg excitation. Assignments and transition energies are listed in Table 5. These assignments are based upon those given by Whetten et al. [17,18] up to an energy of 7.21 eV. The extension to higher energy takes into account additional exci-tations of the totally symmetric ν_2 or ν_3 modes. In this manner,

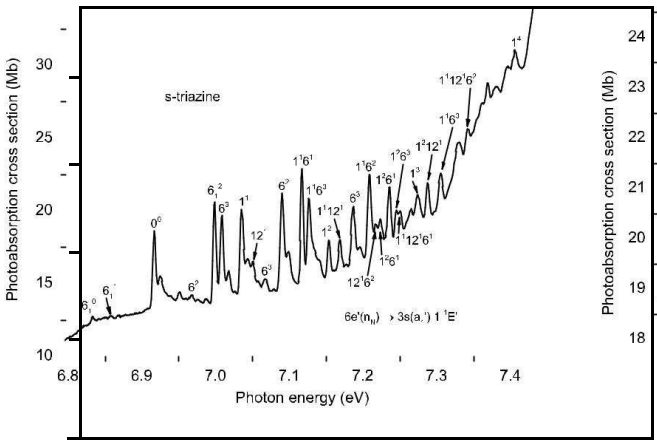

Fig. 4. Photoabsorption cross section of s-triazine, encompassing the excitation range 6.80–7.45 eV, showing structure due to the $6e^0(n_N)$? $3s(a^0_1)$ 1 $^1E^0$ transition. Experimental excitation energies and assignments are given in Table 5.

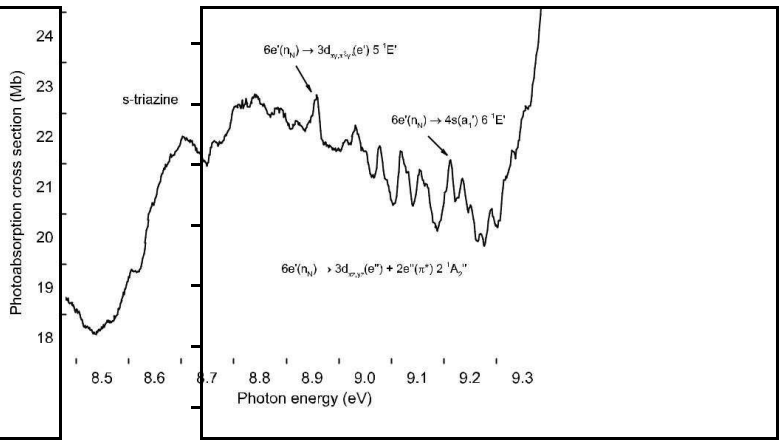

Fig. 5. Photoabsorption cross section of s-triazine, encompassing the excitation range 8.5–9.3 eV, showing structure due to Rydberg states belonging to series converging onto the X $\tilde{E}$ state threshold.

Table 5
Excitation energies and vibrational assignments for absorption bands observed in the $6e^0$? $3s(a^0_1)$ 1 $^1E^0$ Rydberg transition in s-triazine.

Excitation energy (eV)	Vibrational assignment[a]	Excitation energy (eV)	Vibrational assignment[a]
6.833	6_1^0	7.127	$1_0^1 6_0^3$(7/2)
6.858	6_1^1 (3/2+)	7.154	1_0^2
6.868		7.168	$1_0^2 12_0^1$
6.916	0_0^0	7.186	6_0^3 (1/2)
6.924		7.208	$1_0^1 6_0^2$ (1/2)
6.950		7.221	$12_0^1 6_0^2$ (1/2)
6.968	6_0^2 (5/2)	7.235	$1_0^2 6_0^1$ (1/2)
6.999	6_1^2 (1/2)	7.245	$1_0^2 6_0^3$ (7/2)
7.008	6_0^3	7.250	$1_0^1 12_0^1 6_0^1$ (1/2)
7.017		7.274	1_0^3
7.035	1_0^1	7.288	$1_0^2 12_0^1$
7.043		7.305	$1_0^1 6_0^3$ (1/2)
7.050	12_0^1	7.329	
7.067	6_0^3 (5/2)	7.342	$1_0^1 12_0^1 6_0^2$ (1/2)
7.090	6_0^2 (1/2)	7.369	
7.098		7.406	1_0^4
7.117	$1_0^1 6_0^1$ (1/2)		

[a] The half integer number in parentheses is the quantum number j which char-acterises the eigenstate [18].

most of the observed peaks can be assigned and associated with the 3s Rydberg state. Of the remaining unidentified peaks, several have excitation energies 8 meV higher than those of prominent peaks. This pattern suggests that they could be hot bands. Since our spectrum was recorded with the temperature of the sample molecules being at 40 LC, whereas that of Whetten et al. [17] was recorded with a cooled sample, our spectrum is more likely to exhibit hot bands, possibly involving the low energy $m_{14}(e^{00})$ mode which has an energy of 41.9 meV [47] in the neutral ground state. At energies below the peak due to the adiabatic transition, several weak bands are ascribed to hot band excitations [17,18].

Walker et al. [6] suggest that structure occurring at 7.97 and 8.161 eV in their absorption spectrum should be assigned to the $6e^0$? 3p and $6e^0$? 3d transitions, respectively. Our spectrum (Fig. 3) exhibits weak but broad structure, including a shoulder at 7.98 eV, superimposed upon the intense absorption band cen-tred around 7.8 eV. However, there is no evidence of the vibra-tional structure which might be expected of a transition into a Rydberg state. Our calculations predict that the $6e^0$? $3p_{x,y}(e^0)$ and $6e^0$? $3d_{z^2}$ (a^0_1) transitions occur in the region of the main intense band but we conclude that ascribing specific features to those Rydberg excitations is questionable.

In the energy range between 8.5 and 9.3 eV the photoabsorption spectrum (Fig. 5) contains a very broad band with superimposed structure. This structure is noticeably sharper at energies above 8.9 eV than below. As already mentioned, the broad band may be due to the $6e^0(n_N)$? $2e^{00}(\pi^*)$ valence transition (Table 4). According to our calculations, three states, namely 5 $^1E^0$, 2 $^1A^{00}_2$ and 6 $^1E^0$, have excitation energies between 8.8 and 9.1 eV. Of these states, the 5 $^1E^0$ and 6 $^1E^0$ are principally Rydberg states and correspond to the $6e^0$? $3d_{xy,x^2-y^2}$ (e^0) and $6e^0$? $4s(a^0_1)$ transitions, respectively. The 2 $^1A^{00}_2$ state has a mixed Rydberg/valence character with the Rydberg contribution arising from the $6e^0$? $3d_{xz,yz}(e^{00})$ transition. The vibrational structure associated with these Rydberg states is broader than that associated with the $3sa^0_1$ state, possibly as a result of Rydberg/valence mixing. Nevertheless, if the peak at 8.907 eV is assumed to correspond to the adiabatic transition into the 5 $^1E^0$ state, whose calculated excitation energy is 8.80 eV (Table 4), then some of the vibrationally excited peaks are sepa-rated from the adiabatic peak by intervals similar to those in the 3s state band. Excitation energies for some of the structure are given in Table 6. The peak at 9.161 eV does not appear to belong to the vibronic structure associated with the 5 $^1E^0$ state and could, therefore, be assigned to the adiabatic transition into the 6 $^1E^0$ state. A few vibrational peaks, with characteristic energy spacings, are tentatively associated with this second Rydberg state (Table 6).

The next energy range in which the photoabsorption spectrum displays vibrational progressions occurs between 9.3 and 10.5 eV (Fig. 6) and energetic considerations suggest that this structure could be due to either the first member of a Rydberg series converging onto the A $\tilde{E}$ state limit or to a higher member of a Rydberg series converging onto the X $\tilde{E}$ state limit. If it is assumed that the peak observed at 9.372 eV corresponds to the adiabatic transition into a Rydberg state of principal quantum number n = 3, converging onto the $A^{\sim 2}E^{00}$ state ionisation threshold at 11.69 eV [45], then a quantum defect of 0.58 is obtained. Such a value is indicative of a p-type Rydberg series. In support of this suggestion, our calculations predict that the $1e^{00}$? $3p_{x,y}(e^0)$ + $3d_{xy,x^2-y^2}(e^0)$ 5 $^1A^{00}_2$ transition lies at 9.67 eV and has a reasonably high oscillator strength of 0.0409.

The vibrational structure in the A $\tilde{E}$ state photoelectron band has been assigned to a single progression in the $m^+_2(a^0_1)$ mode with

Table 6
Excitation energies and assignments for structure observed in the photoabsorption spectrum of s-triazine.

Assignment	Excitation energy (eV)
$6e^0$? $3d_{xy;x^2\ y^2}$ (e^0) 5 $^1E^0$	8.907 8.963 8.980 8.998 9.026 9.067 9.104 9.116
$6e^0$? 4s $(a_1{}^0)$ 6 $^1E^0$	9.161 9.185 9.200 9.238 9.280
$1e^{00}$? $3p_{x,y}$ (e^0) + $3d_{xy;x^2\ y^2}$ (e^0) 5 $^1A_2{}^{00}$	9.372 9.482 9.504 9.599 9.625 9.704
$1e^{00}$? $4p_{x,y}$ (e^0) + $4d_{xy;x^2\ y^2}$ (e^0) 8 $^1A_2{}^{00}$	10.602 10.730 10.830
$5a_1{}^0$? $3pe^0$, $3pa_2{}^{00}$	10.962 11.051 11.133

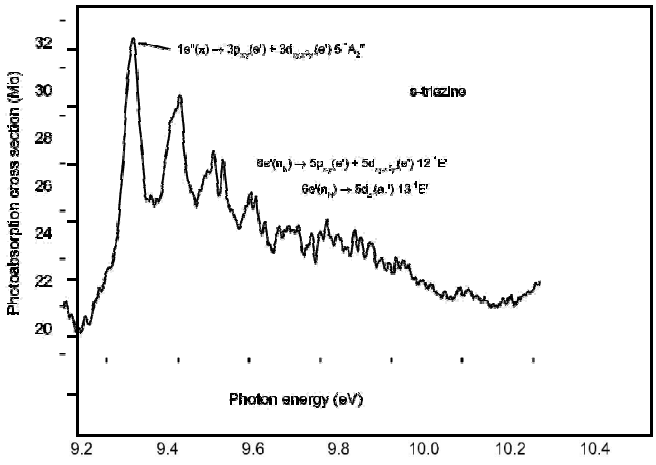

Fig. 6. Photoabsorption cross section of s-triazine, encompassing the excitation range 9.2–10.5 eV, showing structure due to Rydberg states. According to our CCSD predictions (Table 4), the peak observed around 9.4 eV may be associated with the adiabatic transition into the lowest lying Rydberg state involving the $1e^{00}(p)$ orbital. Calculated transition energies for the 5 $^1A^{00}_2$, 12 $^1E^0$ and 13 $^1E^0$ states are given in Table 4.

an energy of 122 meV [45]. As has been discussed in relation to the $\tilde{X}\ ^2E$ state, Jahn-Teller interactions may be expected to affect the vibronic levels in this degenerate state. The structure observed in our absorption spectrum (Fig. 6) exhibits a greater complexity than that in the photoelectron spectrum [45]. Even so, a few of the vibrational peaks are separated by intervals which recur, and these are listed in Table 6. To a certain extent it can be seen that the absorption structure resembles that in the photoelectron spectrum. For example, the absorption band appearing at 9.49 eV, due to the contributions from the first two excited vibronic levels, has a doublet profile with peaks whose energies lie 110 and

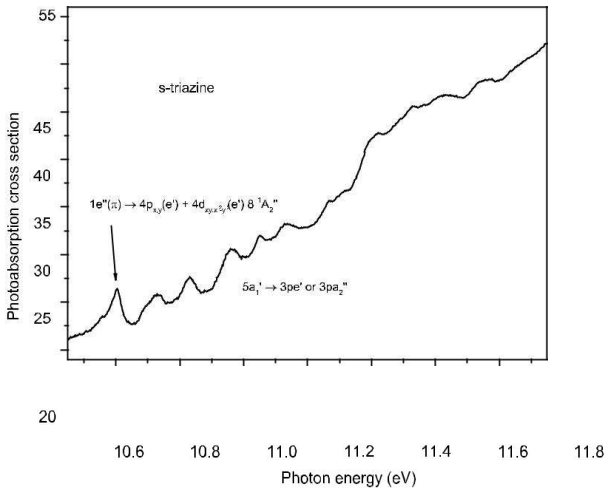

Fig. 7. Photoabsorption cross section of s-triazine encompassing the excitation range 10.5–12.0 eV. The structure above 11 eV may involve excitation from the $5a^0_1$ orbital.

132 meV above the adiabatic threshold. The centre of this doublet correlates approximately with the vibrational spacing of 122 meV observed in the photoelectron spectrum [45].

The width of the $\tilde{A}\ ^2E$ state photoelectron band vibrational envelope (0.5 eV) is approximately half that of the absorption structure which, to this point, has been discussed solely in terms of the 5 $^1A^{00}_2$ state. However, it is possible that the absorption bands at the high energy end of this structure belong to an additional Rydberg state and according to our theoretical results the 12 $^1E^0$ and 13 $^1E^0$ states due to the $6e^0$? $5p_{x,y}(e^0)$ + $5d_{xy;x^2\ y^2}$ (e^0) and $6e^0$? $5d_{z^2}$ (a^0_1) transitions, respectively, lie at 9.80 and 9.88 eV.

The n = 4 member of the $1e^{00}$? $np_{x,y}(e^0)$ + $nd_{xy;x^2\ y^2}$ (e^0) series, corresponding to the 8 $^1A^{00}_2$ state, has a calculated transition energy of 10.85 eV and an oscillator strength of 0.0162 (Table 4). Thus this Rydberg state might be associated with one or more of the broad bands appearing in the photoabsorption spectrum between 10.5 and 12.0 eV (Fig. 7).

An alternative interpretation for all, or at least some, of the absorption bands in this region, is that they are due to Rydberg states belonging to series converging onto the $(5a_1)$ B A_1 state ionisation limit at 13.26 eV [45]. The corresponding photoelectron band exhibits a single vibrational progression, containing three members, in the $m^+_2(a^0_1)$ mode [45]. Electric-dipole selection rules allow npe^0, na^{00}_2 and nde^0 Rydberg series following excitation from the $5a^0_1$ orbital. Assuming that the peak at 10.602 eV corresponds to the adiabatic transition into an n = 3 state, then the derived quantum defect is 0.74. This value is slightly larger than expected for a p-series. Another prominent peak occurs at 10.962 eV, and the associated quantum defect of 0.57 falls within the normal range for such a series. Thus, our tentative interpretation of the absorption bands observed between 10.5 and 12.0 eV is that those in the lower energy region belong to the 8 $^1A^{00}_2$ state, whilst those at higher energy are due to $5a^0_1$? $3pe^0$ or $3pa^{00}_2$ excitations (Table 6). The unusually broad vibrational peaks associated with this absorption structure suggest strong mixing occurs between the Rydberg and valence states.

5. Summary

Synchrotron radiation has been used to measure the absolute photoabsorption cross section of s-triazine between 4 and 40 eV. The spectrum is dominated by broad bands due to

transitions into valence states. The overlapping contributions from the calculated low-lying $6e^0(n_N)$? $3p_{x,y}(e^0)$ and $1e^{00}(p)$? $2e^{00}(p')$ $^1E^0$ transitions at 8.12 eV and the $1e^{00}(p)$? $4e^{00}(p')$ $^1E^0$ transition at 8.31 eV give rise in the experiment to an intense band at 7.8 eV. This band is similar to those, mainly due to p ? p' transi-tions, observed in the diazines [2] and benzene [2]. In contrast to the prominent bands due to valence states, the spectrum of s-tri-azine exhibits only weak structure associated with Rydberg excita-tions. The assignment of much of the Rydberg structure is hampered by the irregular intensities and excitation energies of the corresponding absorption bands.

Transition energies and oscillator strengths for Rydberg and valence excitations have been calculated with the TDDFT and cou-pled cluster approaches. The coupled cluster predictions have been used to help interpret the discrete structure due to Rydberg excita-tions observed in the experimental spectrum whilst the TDDFT results provide a satisfactory description of the photoabsorption spectrum over the complete valence shell region. The theoretical studies show that Rydberg/Rydberg and Rydberg/valence mixing is important and that many of the states cannot be described ade-quately in terms of a single-electron excited configuration. It appears that this mixing perturbs the Rydberg states to such an extent that regular series cannot be identified in the experimental spectrum.

The influence of Jahn-Teller effects has been observed in the absorption bands due to excitation from the $1e^{00}$ or $6e^0$ orbitals into Rydberg orbitals. The vibronic structure associated with the $6e^0$? $3sa^0{}_1$ transition has been assigned based upon the results from an earlier two-photon absorption study [17,18].

An improved understanding of the valance shell electronic states of s-triazine necessitates additional experimental and theo-retical studies. On the experimental front, higher resolution photo-electron and photoabsorption spectra would help elucidate the vibronic structure associated with ionisation and excitation, respectively, from the $1e^{00}$ and $6e^0$ orbitals. The presently available HeI excited photoelectron spectra are insufficient to allow the influence of the Jahn-Teller effect to be investigated in a detailed manner. Higher resolution spectra might enable the vibronic struc-ture associated with this effect to be analysed and assigned. This, in turn, could aid the interpretation of a higher resolution photoab-sorption spectrum. Such a spectrum could be recorded using a Fourier transform spectrometer coupled to a source of synchrotron radiation. A facility of this nature has recently allowed high resolu-tion absorption spectra of some five-membered ring-type mole-cules to be obtained [49,50], and is well suited to the study of small polyatomic molecules. A high resolution photoabsorption spectrum of s-triazine might enable the structure due to the Jahn-Teller effect to be observed and identified in some of the higher-lying electronic states, as has already been achieved for the $6e^0$? $3sa^0{}_1$ $^1E^0$ transition [17,18]. The observation and assign-ment of the vibronic structure associated with the Jahn-Teller effect, in both the photoabsorption and the photoelectron spectra, is probably a crucial step towards improving our understanding of the valence shell electronic structure.

Since the vibronic structure occurring in an absorption band corresponding to a Rydberg state should resemble that in the pho-toelectron band associated with the ionisation threshold onto which the Rydberg series converges, experimental studies per-formed with sufficient resolution should enable the Rydberg state to be identified. This would help overcome a difficulty encountered in the present lower resolution work where, in some instances, it has not been possible to decide whether a particular absorption band should be assigned to a low-n Rydberg state arising from excitation of the $1e^{00}$ orbital or to a high-n Rydberg state arising from excitation of the $6e^0$ orbital.

From the purely theoretical point of view, the density of states becomes very high at transition energies above the low-lying exci-tations and it then becomes complicated to provide a full assign-ment at the single state level. Even highly advanced ab initio approaches, which go beyond the single excitation space included in the TDDFT method, show some energy shift, and it is difficult to have an exact balance of correlation between the valence and Ryd-berg states, as well as ensuring that the basis set is saturated. Sim-ulation of the vibrational structure, including that due to the Jahn-Teller effect, may prove important, and further advancement in theoretical approaches is expected to provide a more comprehen-sive assignment for some of the higher-lying states.

Acknowledgement

S.C. acknowledges support from the AIAS-COFUND Marie-Curie programme (grant number 609033).

References

[1] M. Stener, P. Decleva, D.M.P. Holland, D.A. Shaw, J. Phys. B 44 (2011) 075203.
[2] D.M.P. Holland, D.A. Shaw, S. Coriani, M. Stener, P. Decleva, J. Phys. B 46 (2013) 175103.
[3] M.R. Silva-Junior, M. Schreiber, S.P.A. Sauer, W. Thiel, J. Chem. Phys. 129 (2008) 104103.
[4] S.P.A. Sauer, M. Schreiber, M.R. Silva-Junior, W. Thiel, J. Chem. Theory Comput. 5 (2009) 555.
[5] M.R. Silva-Junior, M. Schreiber, S.P.A. Sauer, W. Thiel, J. Chem. Phys. 133 (2010) 174318.
[6] I.C. Walker, M.H. Palmer, C.C. Ballard, Chem. Phys. 167 (1992) 61.
[7] S. Coriani, M. Stener, P. Decleva, D.M.P. Holland, A.W. Potts, L. Karlsson, Chem. Phys. 450 (2015) 115.
[8] K.K. Innes, I.G. Ross, M.R. Moomaw, J. Mol. Spectrosc. 132 (1988) 492.
[9] J.S. Brinen, R.C. Hirt, R.G. Schmitt, Spectrochim. Acta 18 (1962) 863.
[10] Y. Udagawa, M. Ito, S. Nagakura, J. Mol. Spectrosc. 39 (1971) 400.
[11] J.D. Webb, K.M. Swift, E.R. Bernstein, J. Chem. Phys. 73 (1980) 4891.
[12] M. Heaven, T. Sears, V.E. Bondybey, T.A. Miller, J. Chem. Phys. 75 (1981) 5271.
[13] A. Bolovinos, P. Tsekeris, J. Philis, E. Pantos, G. Andritsopoulos, J. Mol. Spectrosc. 103 (1984) 240.
[14] P.U. de Haag, W.L. Mearts, J.T. Hougen, Chem. Phys. 151 (1991) 371.
[15] T.A. Barckholtz, T.A. Miller, Int. Rev. Phys. Chem. 17 (1998) 435.
[16] V.A. Mozhayskiy, A.I. Krylov, Mol. Phys. 107 (2009) 929.
[17] R.L. Whetten, E.R. Grant, J. Chem. Phys. 81 (1984) 691.
[18] R.L. Whetten, K.S. Haber, E.R. Grant, J. Chem. Phys. 84 (1986) 1270.
[19] D.M.P. Holland, D.A. Shaw, I.C. Walker, I.J. McEwen, M.F. Guest, Chem. Phys. 344 (2008) 227.
[20] D.A. Shaw, D.M.P. Holland, M.A. MacDonald, A. Hopkirk, M.A. Hayes, S.M. McSweeney, Chem. Phys. 163 (1992) 387.
[21] D.M.P. Holland, Phys. Scrip. 36 (1987) 22.
[22] D.M.P. Holland, J.B. West, A.A. MacDowell, I.H. Munro, A.G. Beckett, Nucl. Instrum. Methods B44 (1989) 233.
[23] D.M.P. Holland, D.A. Shaw, I.C. Walker, I.J. McEwen, M.F. Guest, J. Phys. B 42 (2009) 035102.
[24] D.M.P. Holland, D.A. Shaw, A. Hopkirk, M.A. MacDonald, S.M. McSweeney, J. Phys. B 25 (1992) 4823.
[25] M.E. Casida, in: D.P. Chong (Ed.), Recent Advances in Density Functional Methods, World Scientific, Singapore, 1995, p. 155.
[26] S.J.A. Van Gisbergen, J.G. Snijders, E.J. Baerends, Comput. Phys. Commun. 118 (1999) 119.
[27] M. Stener, G. Fronzoni, P. Decleva, J. Chem. Phys. 122 (2005) 234301.
[28] P. Decleva, M. Stener, D.M.P. Holland, A.W. Potts, L. Karlsson, J. Phys. B 40 (2007) 2939.
[29] R. Van Leeuven, E.J. Baerends, Phys. Rev. 49 (1994) 2421.
[30] S.J.A. Van Gisbergen, V.P. Osinga, O.V. Gritsenko, R. Van Leeuven, J.G. Snijders, E.J. Baerends, J. Chem. Phys. 105 (1996) 3142.
[31] M. Stener, S. Furlan, P. Decleva, J. Phys. B 33 (2000) 1081.
[32] N. Kishimoto, K. Ohno, J. Phys. Chem. A 104 (2000) 6940.
[33] O. Christiansen, P. Jørgensen, C. Hättig, Int. J. Quant. Chem. 68 (1998) 1.
[34] G.D. Purvis, R.J. Bartlett, J. Chem. Phys. 76 (1982) 1910.
[35] R.A. Kendall, T.H. Dunning, R.J. Harrison, J. Chem. Phys. 96 (1992) 6796.
[36] O. Christiansen, H. Koch, P. Jørgensen, J. Chem. Phys. 105 (1996) 1451.
[37] K. Kaufmann, W. Baumeister, M. Jungen, J. Phys. B 22 (1989) 2223.
[38] K. Aidas, C. Angeli, K.L. Bak, V. Bakken, R. Bast, L. Boman, O. Christiansen, R. Cimiraglia, S. Coriani, P. Dahle, E.K. Dalskov, U. Ekstroem, T. Enevoldsen, J.J. Eriksen, P. Ettenhuber, B. Fernandez, L. Ferrighi, H. Fliegl, L. Frediani, K. Hald, A. Halkier, C. Haettig, H. Heiberg, T. Helgaker, A.C. Hennum, H. Hettema, E. Hjertenæs, S. Høst, I.-M. Høyvik, M.F. Iozzi, B. Jansik, H.J.Aa. Jensen, D. Jonsson, P. Jørgensen, M. Kaminski, J. Kauczor, S. Kirpekar, T. Kjærgaard, W. Klopper, S. Knecht, R. Kobayashi, H. Koch, J. Kongsted, A. Krapp, K. Kristensen, A. Ligabue,

O.B. Lutnaes, J.I. Melo, K.V. Mikkelsen, R.H. Myhre, C. Neiss, C.B. Nielsen, P. Norman, J. Olsen, J.M.H. Olsen, A. Osted, M.J. Packer, F. Pawlowski, T.B. Pedersen, P.F. Provasi, S. Reine, Z. Rinkevicius, T.A. Ruden, K. Ruud, V. Rybkin, P. Salek, C.C.M. Samson, A. Sanchez de Meras, T. Saue, S.P.A. Sauer, B. Schimmelpfennig, K. Sneskov, A.H. Steindal, K.O. Sylvester-Hvid, P.R. Taylor, A.M. Teale, E.I. Tellgren, D.P. Tew, A.J. Thorvaldsen, L. Thøgersen, O. Vahtras, M. A. Watson, D.J.D. Wilson, M. Ziolkowski, H. Ågren, WIREs Comput. Mol. Sci. 4 (2014) 269.

[39] R.S. Prasad, B.N. Rai, Theor. Chim. Acta 77 (1990) 343.
[40] J.E. Del Bene, J.D. Watts, R.J. Bartlett, J. Chem. Phys. 106 (1997) 6051.
[41] D.P. Chong, Can. J. Chem. 87 (2009) 1148.
[42] M.B. Robin, Higher Excited States of Polyatomic Molecules, vol. 1, Academic Press, New York, 1974.
[43] E. Lindholm, Ark. Fysik 40 (1968) 97.
[44] C.E. Theodosiou, M. Inokuti, S.T. Manson, At. Data Nucl. Data Tables 35 (1986) 473.

[45] C. Fridh, L. Åsbrink, B.Ö. Jonsson, E. Lindholm, Int. J. Mass Spectrom. Ion Phys. 8 (1972) 85.
[46] G. Herzberg, Molecular Spectra and Molecular Structure, Infrared and Raman Spectra of Polyatomic Molecules, Vol. II, Van Nostrand Reinhold, New York, 1945.

[47] A.D. Boese, J.M.L. Martin, J. Phys. Chem. A 108 (2004) 3085.
[48] P.J. Larkin, M.P. Makowski, N.B. Colthup, Spectrochim. Acta A55 (1999) 1011.
[49] D.M.P. Holland, A.B. Trofimov, E.A. Seddon, E.V. Gromov, T. Korona, N. de Oliveira, L.E. Archer, D. Joyeux, L. Nahon, Phys. Chem. Chem. Phys. 16 (2014) 21629.
[50] D.M.P. Holland, E.A. Seddon, A.B. Trofimov, E.V. Gromov, M. Wormit, A. Dreuw, T. Korona, N. de Oliveira, L.E. Archer, D. Joyeux, J. Mol. Spectrosc. 315 (2015) 184.